HHS Public Access

Author manuscript

Mol Imaging Biol. Author manuscript; available in PMC 2022 March 29.

Published in final edited form as:

Mol Imaging Biol. 2020 February ; 22(1): 144–155. doi:10.1007/s11307-019-01434-2.

Comparison of A Short Versus Long Stokes Shift Near-Infrared Dye During Intraoperative Molecular Imaging

Christopher J. Corbett[1], **Lydia G. Frenzel Sulyok**[1], **Jarrod D. Predina**[1], **Andrew D. Newton**[1], **Mitchell G. Bryski**[1], **Leilei Xia**[1], **Jason Stadanlick**[1], **Michael H. Shin**[1], **Sakkarapalayam M. Mahalingam**[2,3], **Philip S. Low**[2], **Sunil Singhal**[1]

[1]Perelman School of Medicine at the University of Pennsylvania, 3400 Civic Center Blvd. Philadelphia, PA 19104

[2]Purdue University Department of Chemistry, 560 Oval Drive, West Lafayette, IN 47907

[3]Department of Chemistry, SRM Institute of Science and Technology, Kattankulathur, Kancheepuram 603203, Tamilnadu, India

Abstract

Purpose: Intraoperative molecular imaging (IMI) utilizes optical dyes that accumulate within tumors to assist with detection during a cancer operation. IMI can detect disease not visualized preoperatively, as well as positive margins. However, these dyes are limited by autofluorescence, signal reflection, and photon-scatter. We hypothesize a novel dye with a wide separation between excitation and emission spectra, SS180, would help overcome these obstacles.

Procedures: Two targeted molecular contrast agents, OTL38 and SS180, were selected for this study. Both dyes had the same targeting ligand to folate receptor alpha (FRα). OTL38, a well-annotated IMI agent in human trials, has a Stokes Shift of 22 nm, whereas SS180, the new dye, has a Stokes Shift of 129 nm. Cell lines were tested for FRα expression and incubated with dyes to demonstrate receptor-dependent binding. Cells were incubated in various concentrations of the dyes to compare dose- and time-dependent binding. Finally, cells tagged with the dyes were injected subcutaneously in a murine model to estimate tumor burden necessary to generate fluorescent signal.

Results: Cellular studies demonstrated SS180 binds cells in a dose-, receptor-, and time-dependent manner, and exhibited higher mean fluorescence intensities by flow cytometry when compared with OTL38 for each time point and concentration. In an *in vivo* flank tumor model, SS180 had a higher tumor to background ratio (TBR) than OTL38, though not statistically significant ($p = 0.08$). *Ex vivo*, OTL38 had a higher TBR than SS180 ($p = 0.02$). The subcutaneous

Corresponding Author: Christopher Corbett, chris.j.corbett.13@gmail.com, Telephone: 215-662-4767, Fax: 215-615-6562.

Conflicts of Interest

Philip Low is on the Board of Directors at On Target Laboratories, manufacturers of all study drugs utilized in this report. The remaining authors declare that they have no conflict of interest.

model revealed SS180 had a higher TBR at 5×10^6 cells than OTL38 ($p = 0.05$). No toxicity was observed in the animals.

Conclusions: SS180 exhibits greater TBRs *in vivo*, but not *ex vivo*. These findings suggest SS180 may have weaker fluorescence, but superior contrast. Studies in large animal models and clinical trials may better elucidate the clinical value of a long Stokes Shift.

Keywords

Oncology; Surgery; Imaging; Fluorescence; Small-Molecule; Dye

Introduction

Cancer remains the second most common cause of death in the United States despite continued advances in medical and surgical management [1]. In 2019, there will be an estimated 1.76 million new cancer diagnoses and over 600,000 deaths [1]. Surgery remains one of the best opportunities for curing patients with solid malignancies [2]. Despite surgical interventions, many patients develop local or systemic recurrences that significantly worsen survival [3]. Often these recurrences are due to residual disease, either from positive surgical margins or microscopic, multifocal disease that cannot be detected by the surgeon at the time of the operation [4]. Rates of positive surgical margins in many solid malignancies have failed to improve over the last several decades [4]. Additionally, surgeons depend on preoperative imaging modalities such as Positron Emission Tomography (PET) and X-ray Computed Tomography (CT) scans to locate tumors; however, they lack sensitivity for small nodules [5,6]. Thus, even with advances in medical and surgical management, the surgeon is limited in their ability to know about all disease prior to the operation or to completely resect known disease.

Intraoperative molecular imaging (IMI) is a potential adjunct to the operating surgeon that can allow for real-time identification of multifocal disease and margin assessment [7]. IMI can improve complete surgical resection rates, decrease local recurrence, and consequently has the potential to cure more patients [7]. IMI consists of two key components: a targeted, fluorescent dye that localizes to the tumor, and an imaging system that allows for real-time detection of the fluorescent signal without interrupting the surgeon's workflow. This assessment happens in real-time and can be used in minimally invasive procedures to further aid the surgeon who cannot palpate tissue to assess for malignancy. IMI has been utilized for multiple types of solid malignancies, including lung, bladder, and breast cancers [7–9]. Importantly, IMI has been shown to address some of the shortcomings of current surgical management [10].

Dyes used for IMI of lung cancer have gone through several iterations, each addressing the shortcomings of prior generations. Indocyanine green (ICG) has been used for over a decade in IMI but has poor specificity. It localizes to the tumor through leaky vasculature, termed the enhanced permeability and retention (EPR) effect, and will also accumulate in areas of inflammation or infection [9]. The poor specificity of ICG was overcome by targeting receptors upregulated in lung cancers. FRα is upregulated in pulmonary adenocarcinomas, has increased receptor density compared with normal lung parenchyma, and is also present

in a majority of local and distant metastases [11–14]. Our group has assessed the ability of two FRα-targeted dyes to identify pulmonary adenocarcinoma: EC17 and OTL38.

EC17, the first FRα-targeted dye assessed, has excitation and emission spectra that peak at 470 nm and 520 nm, respectively [15]. IMI with EC17 can accurately detect positive margins with a sensitivity of 80%, specificity of 100%, positive predictive value of 100% and negative predictive value of 83% [16]. While early findings in human trials were promising, further research demonstrated that EC17's fluorescent signal was compromised *in vivo* by autofluorescence and poor depth of penetration, likely due to its excitation and emission spectra falling within the visible spectrum [16,17]. OTL38 was developed to overcome these limitations. This contrast agent has excitation and emission spectra that peak at 774 nm and 794 nm, respectively, which both fall into the near infrared (NIR) range [15]. Using OTL38, IMI detected lesions as small as 2 mm, much smaller than what can be detected with preoperative cross-sectional imaging [18]. Similar to EC17, pre-clinical models and early clinical trials with OTL38 helped identify lung adenocarcinomas with sensitivities approaching 100% [18]. Together, these attributes make IMI an attractive adjunct to improve surgical outcomes in patients with cancer. However, false-positive signal with OTL38 was encountered, as in the case of granulomas [18]. While resection of false positives is more acceptable than failure to resect false negatives as it relates to cancer, this signifies there is still room to improve on existing dyes.

Like EC17 and OTL38, SS180 is targeted to FRα and contains the identical ligand. While EC17 uses fluorescein isothiocyanate as its fluorophore, both OTL38 and SS180 utilize a cyanine backbone dye [15]. However, EC17 and OTL38 both exhibit small Stokes Shifts of 50 nm and 20 nm, respectively, while a small change in the molecular structure of the component connecting the fluorophore and ligand in SS180 results in a much larger Stokes Shift of 129 nm. This wider difference between the peak excitation and emission wavelengths theoretically should allow for better differentiation of the spectra and generation of a cleaner fluorescence signal by eliminating issues such as reflection and autofluorescence. Therefore, our goal was to compare SS180 with OTL38 in established cell lines and murine flank tumor models to assess the optimum administration of SS180. We hypothesize that the unique excitation and emission spectra of SS180, a novel FRα-targeted dye, will improve fluorescence signal quality compared to existing dyes.

Materials and Methods

Please see the Electronic Supplementary Materials for details on methodology for all experiments and data analysis.

Results

Optical Properties of SS180 and OTL38

Prior to evaluating OTL38 and SS180 (Fig. 1) in the cell and murine models, we confirmed the optical properties of both dyes and optimized their detection on the IVIS for subsequent analysis. First, excitation and emission spectra were obtained on a fluorometer (Fig. 2a), which determined that OTL38 had peak excitation and emission spectra at 773 nm and

795 nm, resulting in a Stokes Shift of 22 nm. SS180 had peak excitation and emission spectra at 612 nm and 741 nm, resulting in a Stokes Shift of 129 nm. After determining the peak excitation and emission spectra, fluorescence intensity was assessed using the peak excitation and emission wavelengths for SS180 and OTL38, on serial dilutions ranging from 3.91×10^{-8} to 1×10^{-5} M. The trials were run in triplicate. The fluorescence of DPBS was measured for each set of fluorescence parameters to use as the background readings and were 1.04 at the SS180 parameters and 15.97 at the OTL38 parameters. Readings were then normalized to the fluorescence of DPBS and averaged to yield a peak signal to background ratio (SBR) of 437 for SS180 and 54 for OTL38 ($p < 0.0001$) (Fig. 2b). Finally, we assessed serial dilutions using the IVIS to maximize the SBR of SS180 and OTL38, relative to DPBS, to ensure optimal signal detection in the murine experiments (Fig. 2c), with the optimal excitation and emission parameters for SS180 and OTL38 being 640/780 nm and 745/800 nm respectively. Due to the limitations of the excitation and emission parameters of the IVIS, a correction factor was used to further assess whether SS180 performed superiorly compared with OTL38. At the highest concentrations, OTL38 had a SBR ranging from 2.3 to 4.3 times greater than that of SS180 at their respective, optimized IVIS excitation and emission parameters. As a result, 2 was used as the correction factor, an underestimate of what was observed in the IVIS dye optimization, to better assess whether SS180 had superior *in vivo* fluorescence signal or binding properties.

In Vitro Analysis

Using a library of murine and human cancer cell lines, we set out to optimize the detection of SS180 and OTL38. First, tumors of each cell line were grown in athymic nude mice, were harvested, formalin-fixed, paraffin embedded, sectioned, and stained for FRα (Fig. 3a). We observed variable expression of FRα during the immunohistochemical analysis. These cell lines were then incubated in media spiked with SS180 and processed for fluorescence microscopy and flow cytometry, both of which demonstrated fluorescence that correlated with FRα expression as determined by immunohistochemistry (Fig. 3a).

Next, we set out to determine peak fluorescence for both SS180 and OTL38 using cellular models. Using KB cells, which exhibited the highest expression of FRα, we incubated cells in media spiked with SS180 or OTL38 at concentrations of 1 μM, 2 μM, 5 μM, and 10 μM for up to 24 hours. The fluorescence microscope, with filters specified to both dyes, detected membrane binding of SS180 and OTL38 in a dose- and time-dependent manner (Fig. 3b, 3c). Similarly, flow cytometry showed increases in MFI that exhibited similar trends, with plateauing of the MFI occurring after 8 hours (Fig. 3d). Additionally, across all concentrations and time points, SS180 had a consistently higher MFI.

In Vivo Analysis

Following the cellular studies, we assessed the efficacy of SS180 compared with OTL38 in a murine flank tumor model. As OTL38 and SS180 are both renally excreted, we used a subcutaneous tumor model on the scruff of the neck. 1×10^{6} KB cells were subcutaneously injected, and tumors were monitored until they reached a volume of 500 mm^3. Mice then received a tail vein injection of 100 μl of SS180 or OTL38 in concentrations of 1 μM, 2 μM, 5 μM, or 10 μM. Control mice were injected with DPBS without dye. Mice were

subsequently imaged immediately and at 0.5, 1, 2, 4, 8 and 24 hours after injection at the optimum excitation and emission parameters, 745/800 nm for OTL38 and 640/780 nm for SS180. Images were then processed on ImageJ, with the mean signal intensity of the tumor divided by the mean signal intensity of normal tissue immediately surrounding the tumor to generate the TBR (Fig. 4a). We observed peak TBRs in SS180 at 8 hours and at 24 hours for OTL38, though the peak TBR for SS180 was not significantly greater than that of OTL38 ($p = 0.0806$) (Fig. 4b).

After the mice were imaged at 24 hours, tumors and muscle were harvested. The tumors were then imaged *ex vivo* on the IVIS, and TBRs were subsequently calculated, using the control tumor as reference. We calculated peak TBRs of 4.59 for mice treated with OTL38 and 2.64 for mice treated with SS180 ($p = 0.0210$) (Fig. 4c). Notably, dosing above 5 μM did not result in an increased TBR *ex vivo* for SS180 ($p = 0.7148$). Following *ex vivo* analysis, tumors and muscle were embedded in O.C.T. and sectioned. Slides were then imaged which revealed both SS180 and OTL38 localized to the tumor, but not to healthy muscle (Fig. 4d). Sections were also imaged on the fluorescence microscope, which demonstrated the dye localized to the cell membrane of the tumor cells, and not just to the periphery of the tumor.

Biodistribution and Toxicity

Following assessment of OTL38 and SS180 in the flank tumor model, we treated several more mice with flank tumors with SS180 and OTL38 to assess biodistribution and systemic toxicity. Mice with flank tumors were euthanized 24 hours after receiving 100 μl of 10 μM solutions of OTL38, SS180 or pure DPBS. Tumors and healthy tissue were harvested, including heart, lung, adipose, liver, spleen, stomach, kidneys, small intestine and large intestine. In the control mice, liver, stomach, and large intestine all exhibited fluorescence at the fluorescence parameters for both OTL38 and SS180. Mice receiving both OTL38 and SS180 exhibited significant fluorescence in the kidneys and the tumor (Fig. 5).

Dye Sensitivity Analysis

Next, we sought to determine the ability of SS180 and OTL38 to detect microscopic levels of disease. KB cells were incubated in media spiked with OTL38 or SS180 at a concentration of 10 μM, were counted, and injected subcutaneously in amounts up to 5×10^6 cells in 50 μl (Fig. 6a). Mice were then imaged on the IVIS using the optimal excitation and emission parameters and images were processed using ImageJ to calculate TBRs (Fig. 6b). TBRs greater than 2 were observed when 5×10^6 cells were injected, 2.67 for SS180 and 2.03 for OTL38 ($p = 0.05$).

Next, we investigated how diluting fluorescently labeled cells with unlabeled cells altered the fluorescence intensity. 1×10^6 cells labeled with SS180 or OTL38 were injected subcutaneously in 50 μl alone, or diluted with 1×10^6, 2×10^6 or 3×10^6 unlabeled cells. Mice were imaged on the IVIS at the optimal parameters and processed using ImageJ to determine TBRs. Notably, SS180 had a higher TBR at 1×10^6 cells, 2.18, compared with OTL38, 1.90 ($p = 0.049$) (Fig. 6c). Compared with the diluted labeled cells, 1×10^6 SS180 cells had higher TBRs than when diluted with 3×10^6 cells (TBR = 2.18 vs. 1.73, $p = 0.0322$), 2×10^6 cells (2.18 vs. 1.48, $p = 0.0005$) and 1×10^6 cells (2.18 vs. 1.73, $p = 0.0103$). In contrast, the TBR

did not change significantly when OTL38 labeled cells were diluted with 3×10^6 cells (TBR = 1.90 vs. 1.97, p = 0.617), 2×10^6 cells (1.90 vs. 1.71, p = 0.1635) and 1×10^6 cells (1.90 vs. 1.79, p = 0.2818).

Lastly, depth of penetration of OTL38 and SS180 fluorescence signal was evaluated using a phantom tumor model consisting of agarose and gelatin (Fig. 6d). This model assessed the signal strength of dye-spiked agarose at 2 mm, 7 mm, and 12 mm from the surface for both dyes. The strongest fluorescence signal for both dyes was detected at 2 mm depth from the surface. Fluorescence signal was not detected in either OTL38 or SS180 12 mm from the surface. At 2 mm from the surface, OTL38 exhibited fluorescence signal that was significantly greater than that of SS180 (19.41 vs. 5.91, p = 0.0159). There was almost no difference in fluorescence signal intensity at a depth of 7 mm (1.92 vs. 1.82, p = 0.8696) (Fig. 6e).

Discussion

IMI can accurately detect positive surgical margins and locate multifocal disease not visualized on preoperative imaging. As IMI becomes more widely researched and approaches widespread adoption in the operating room, new camera systems and fluorescent dyes have been developed to overcome IMI's limitations. For pulmonary nodules, ICG, a non-targeted dye, was the first dye studied. EC17, the first targeted molecular imaging agent, improved specificity over ICG. However, its utility was limited by autofluorescence and poor signal differentiation from surrounding tissues due to peak excitation and emission in the visible range of light. OTL38 excites and emits in the NIR range and overcomes these problems. However, false positives and tissue- and photon-scattering make OTL38 imperfect. SS180 attempts to overcome these shortcomings due to its unique Stokes Shift, the gap between the excitation and emission spectra, which is almost six times that of OTL38.

During the analysis of the optical characteristics of SS180 compared with OTL38, we observed a significantly higher peak SBR for SS180. Importantly, though the peak fluorescence intensity at its optimal parameters was higher for OTL38, the background signal, plain DPBS, was also significantly higher. Thus, the corrected SBRs were ultimately greater for SS180. At the exact excitation and emission parameters of OTL38, the small Stokes Shift resulted in significant fluorescent signal from DPBS. We believe this was primarily from signal reflection from the highly overlapping excitation and emission spectra of OTL38. Interestingly, subsequent analysis on the IVIS, where the fluorescence parameters are limited by those used in the device, the emission and detection peaks were 55 nm apart for OTL38. This wider gap decreased the signal intensity of the background and resulted in a higher SBR for OTL38 at its optimal parameters compared with SS180. Due to this limitation, an underestimated correction factor of 2 was used to further assess the calculated TBRs of SS180 to better assess whether this novel dye may function differently *in vivo* and *in vitro* when compared to OTL38, or if all observed differences were due to the baseline increased fluorescence intensity of OTL38, at least when detected by the IVIS.

Prior to assessment in the murine models, we sought to demonstrate FRα binding of SS180. The library of human lung cancer cell lines exhibited variable expression of FRα. In both the fluorescence microscopy and flow cytometric analysis of SS180 binding to these cell lines, we observed increased fluorescent signal with increasing receptor expression and similar increases in MFI with flow cytometry. In a direct comparison with OTL38 in the KB cell line, which exhibited the highest level of FRα expression, we observed receptor saturation after 8 hours of incubation, with minimal increase in MFI after 8 hours. Although the parameters of the flow cytometer match the excitation and emission spectra of SS180 more closely than those of OTL38, we observed higher MFIs at each time point and concentration with SS180 than with OTL38 after being normalized to the same approximate MFI for the negative control. The fluorescent signal similarly increased with increasing incubation concentrations and times as seen on fluorescence microscopy.

The murine flank tumor model exhibited seemingly contradictory findings: *in vivo,* SS180 had a greater TBR at its maximum compared with OTL38, though this was not statistically significant. *Ex vivo*, OTL38 and SS180 both exhibited TBRs greater than 2 that were similar at 5 μM. While doubling the dose of OTL38 resulted in a near doubling of the TBR at a dose of 10 μM, TBRs with SS180 did not increase any further beyond 5 μM. In considering the *in vivo* and *ex vivo* results together, this suggests that autofluorescence and background signal affects the TBR of OTL38, but not in SS180 to the same extent. The removal of surrounding healthy tissues and comparison with a treatment naïve tumor results in a much greater TBR for OTL38, but not SS180 at the highest dosing level.

When accounting for the correction factor in our additional analysis of the *in vivo* and *ex vivo* models employed in this study, there appear to be numerous potential benefits of SS180 compared with OTL38. In the uncorrected, *ex vivo* analysis of flank tumors of mice treated with the two dyes, at the highest dosing, the OTL38 tumors had TBRs of 4.59, compared with 2.64 in mice treated with SS180 (1.7 times greater than OTL8). *In vivo*, the TBR of SS180 treated mice was greater than that of OTL38 treated mice. When taking the correction factor into account, SS180 would have superior fluorescence signal in both of these experiments. This suggests several benefits of SS180. *Ex vivo*, where background signal should no longer be a contributing factor, uncorrected OTL38 TBRs are less than two times greater than that of SS180, which suggests superior accumulation of the dye in tumors compared to tumors with OTL38. *In vivo,* any remaining advantage of the fluorescence intensity of OTL38 is overcome by the minimal background signal of SS180, leading to similar, and in some cases superior fluorescence signal in SS180 treated mice.

The subcutaneous model of fluorescently labeled cells served as a new approach in the assessment and comparison of OTL38 and SS180. One of the major benefits of IMI in clinical scenarios is its ability to detect multifocal disease too small to be detected on preoperative imaging [16, 19]. Though neither dye generated a TBR of greater than 2 until at least 5×10^6 cells were injected, the TBR of SS180 at that volume was significantly greater. Previous assessments of current imaging modalities estimate that 1 cm^3 of tumor contains approximately 1×10^9 cells [5]. IMI with OTL38 has been demonstrated to detect pulmonary nodules as small as 2 mm or 0.008 cm^3 [18]. This equates to just 0.8% of that 1×10^9 cells, or 8 million cells. Five million cells would equate to a lesion even smaller,

or approximately 1.7 mm. Thus, estimates in this subcutaneous model suggest that SS180 could detect sub-centimeter multi-focal disease on a scale at least equivalent, if not greater than that of OTL38. Again, considering the correction factor for the baseline fluorescence intensities of the dyes using the IVIS, the background signal of OTL38 limits its ability to be optimally detected, with SS180's unique spectral characteristics addressing some of these limitations and providing an equivalent, if not superior signal *in vivo,* despite its lower SBR at baseline using these specific IVIS parameters.

The dilutional subcutaneous model hopes to address how reflection may alter the signal intensity in tumors. We also hope to assess the potential for heterogeneous tumors, where only a fraction of the tumor may exhibit upregulation of a specific receptor, to generate a clinically significant signal that can be detected intraoperatively. At pure injections of 1×10^6 labeled cells, SS180 had a significantly greater TBR than OTL38. Once the cells were diluted, we saw a decrease in TBR for SS180 but not for OTL38. Signal reflection and reflection off of nearby tumor cells treated with OTL38 and excited and emitted with a narrower Stokes Shift may ultimately compromise the ability to differentiate healthy tissue from tumor, or in this case labeled and unlabeled tumor.

Finally, depth of penetration remains a constant concern in IMI. In our model, the most superficial collections of dye exhibited significantly higher TBRs with OTL38 than SS180, approximately 3 times greater. The deeper the "lesion" was, the more similar the two dyes TBRs were, with a significantly smaller drop-off in signal intensity observed with SS180 compared with OTL38. Although the baseline signal intensity is greater in OTL38, these findings suggest that SS180 may be relatively superior compared with OTL38 for deeper lesions. Although no fluorescence signal was noted for the deepest collection with either dye, with larger tumors, there may be a depth at which SS180 would be superior to OTL38 for fluorescence signal detection. Ultimately, lesion depth appears to have a greater effect on OTL38 than SS180 fluorescence, suggesting an additional instance where a broad stokes shifts with NIR features may help improve fluorescence imaging.

Two important features of SS180 may explain its improved TBR *in vivo*, but decreased fluorescence when visualized *ex vivo* or in assessing serial concentrations on the IVIS. First, the small change in the chemical structure of SS180 results in a significant change in the Stokes Shift. The Stokes Shift is the difference in the wavelength of excited and emitted light. The emitted light, at a higher wavelength, is consequently at a lower energy. Thus, the change in structure from OTL38 to SS180 results in a greater loss in energy for any photon. This greater loss in energy may also correlate with the efficiency of the dye, or how many excited photons are ultimately emitted. A lower efficiency dye would emit fewer photons, and also decrease the maximum signal intensity. This may account for the smaller maximum fluorescence intensity observed on the fluorometer or in our *ex vivo* tumor analysis but was negated by the increased background reading due to reflection from the narrow Stokes Shift of OTL38.

Second, the chemical structure of SS180 may also result in more avid binding to FRα with less remaining in the surrounding parenchyma. Specifically, the link between the cyanine backbone dye and folate ligand in OTL38 contains a planar benzene ring, while SS180

contains a hydrocarbon chain. The stereochemistry directly adjacent to the folate ligand may alter the binding capacity and properties, ultimately limiting the binding of OTL38 more than SS180. This stereochemical interference would ultimately result in less dye binding to the tumor, with more remaining in the animal or excreted, potentially increasing background signal and decreasing TBR. This may also explain the minimal increase in TBR in doses greater than 5 μM in our *ex vivo* tumor analysis of SS180 as FRα may already be saturated at the lower dose.

Conclusion

IMI has the potential to improve the detection of multifocal disease and real-time margin assessment to assist the surgeon in completely resecting solid tumors and improving the patient's chance at attaining a cure. Here we have described advances and improvements in pre-existing FRα-targeted dyes due to optimized fluorescence parameters of SS180. Though the overall fluorescence intensity and efficiency of SS180 are weaker than that of OTL38, SS180 has decreased reflection and autofluorescence in our cellular and murine flank tumor models. This may be due to the optical or stereochemical properties of the dye. This may ultimately equate to a cleaner, stronger fluorescent signal with less dye administered. OTL38 has already demonstrated promise in clinical trials [18, 20–22]. However, the translation of pre-clinical models does not always correlate in clinical outcomes [23]. Still, its success in these pre-clinical models warrants further investigation. Large animal models of spontaneously occurring lung cancers may help better assess and optimize dosing and the biophysical properties of SS180 before translating to clinical trials.

Supplementary Material

Refer to Web version on PubMed Central for supplementary material.

Acknowledgments

CC was supported by the National Center for Advancing Translational Sciences of the National Institutes of Health under award number TL1TR001880. SS and PL were supported by the National Institutes of Health Biomedical Research Partnership, R01 CA193556. The content is solely the responsibility of the authors and does not necessarily represent the official views of the National Institutes of Health.

References

1. Siegel RL, Miller KD, Jemal A (2019) Cancer statistics, 2019. CA Cancer J Clin. 69:7–34. [PubMed: 30620402]
2. Cronin KA, Lake AJ, Scott S, et al. (2018) Annual Report to the Nation on the Status of Cancer, part I: National cancer statistics. Cancer 124:2785–2800. [PubMed: 29786848]
3. Aliperti LA, Predina JD, Vachani A, Singhal S (2011) Local and systemic recurrence is the Achilles heel of cancer surgery. Ann Surg Oncol 18:603–607. [PubMed: 21161729]
4. Orosco RK, Tapia VJ, Califano JA, et al. . (2018) Positive Surgical Margins in the 10 Most Common Solid Cancers. Sci Rep 8:5686. [PubMed: 29632347]
5. Frangioni JV (2008) New technologies for human cancer imaging. J Clin Oncol 26:4012–4021. [PubMed: 18711192]
6. Erdi YE (2012) Limits of Tumor Detectability in Nuclear Medicine and PET. Mol Imaging Radionucl Ther 21:23–28. [PubMed: 23486256]

7. Newton AD, Kennedy GT, Predina JD, et al. (2016) Intraoperative molecular imaging to identify lung adenocarcinomas. J Thorac Dis 8(Suppl 9):S697–S704. [PubMed: 28066672]
8. Hungerhuber E, Stepp H, Kriegmair M, et al. (2007) Seven years' experience with 5aminolevulinic acid in detection of transitional cell carcinoma of the bladder. Urology. 69:260–264. [PubMed: 17320660]
9. Schaafsma BE, Mieog JS, Hutteman M, et al. (2011) The clinical use of indocyanine green as a near-infrared fluorescent contrast agent for image-guided oncologic surgery. J Surg Oncol 104:323–332. [PubMed: 21495033]
10. Newton AD, Predina JD, Nie S, et al. (2018) Intraoperative fluorescence imaging in thoracic surgery. J Surg Oncol 118:344–355. [PubMed: 30098293]
11. O'Shannessy DJ, Yu G, Smale R, et al. (2012) Folate receptor alpha expression in lung cancer: diagnostic and prognostic significance. Oncotarget 3:414–425. [PubMed: 22547449]
12. Elnakat H, Ratnam M (2004) Distribution, functionality and gene regulation of folate receptor isoforms: implications in targeted therapy. Adv Drug Deliv Rev 56:1067–1084. [PubMed: 15094207]
13. Iwakiri S, Sonobe M, Nagai S, et al. (2008) Expression status of folate receptor alpha is significantly correlated with prognosis in non-small-cell lung cancers. Ann Surg Oncol 15:889–899. [PubMed: 18181001]
14. Boogerd LS, Boonstra MC, Beck AJ, et al. (2016) Concordance of folate receptor-alpha expression between biopsy, primary tumor and metastasis in breast cancer and lung cancer patients. Oncotarget 7:17442–17454. [PubMed: 26943581]
15. De Jesus E, Keating JJ, Kularatne SA, et al. (2015) Comparison of Folate Receptor Targeted Optical Contrast Agents for Intraoperative Molecular Imaging. Int J Mol Imaging 2015:469047.
16. Keating JJ, Okusanya OT, De Jesus E, et al. (2016) Intraoperative Molecular Imaging of Lung Adenocarcinoma Can Identify Residual Tumor Cells at the Surgical Margins. Mol Imaging Biol 18:209–218. [PubMed: 26228697]
17. Okusanya OT, DeJesus EM, Jiang JX, et al. (2015) Intraoperative molecular imaging can identify lung adenocarcinomas during pulmonary resection. J Thorac Cardiovasc Surg 150:28–35 e21. [PubMed: 26126457]
18. Predina JD, Newton AD, Keating J, et al. (2017) Intraoperative Molecular Imaging Combined With Positron Emission Tomography Improves Surgical Management of Peripheral Malignant Pulmonary Nodules. Ann Surg 266:479–488. [PubMed: 28746152]
19. Keating J, Newton A, Venegas O, et al. (2017) Near-Infrared Intraoperative Molecular Imaging Can Locate Metastases to the Lung. Ann Thorac Surg 103:390–398. [PubMed: 27793401]
20. Predina JD, Newton AD, Xia L, et al. (2018) An open label trial of folate receptor-targeted intraoperative molecular imaging to localize pulmonary squamous cell carcinomas. Oncotarget 9:13517–13529. [PubMed: 29568374]
21. Predina JD, Newton AD, Keating J, et al. (2018) A Phase I Clinical Trial of Targeted Intraoperative Molecular Imaging for Pulmonary Adenocarcinomas. Ann Thorac Surg 105:901–908. [PubMed: 29397932]
22. Predina JD, Newton A, Corbett C, et al. (2018) Localization of Pulmonary Ground-Glass Opacities with Folate Receptor-Targeted Intraoperative Molecular Imaging. J Thorac Oncol 13:1028–1036. [PubMed: 29626619]
23. Seok J, Warren HS, Cuenca AG, et al. (2013) Genomic responses in mouse models poorly mimic human inflammatory diseases. Proc Natl Acad Sci USA 110:3507–3512. [PubMed: 23401516]

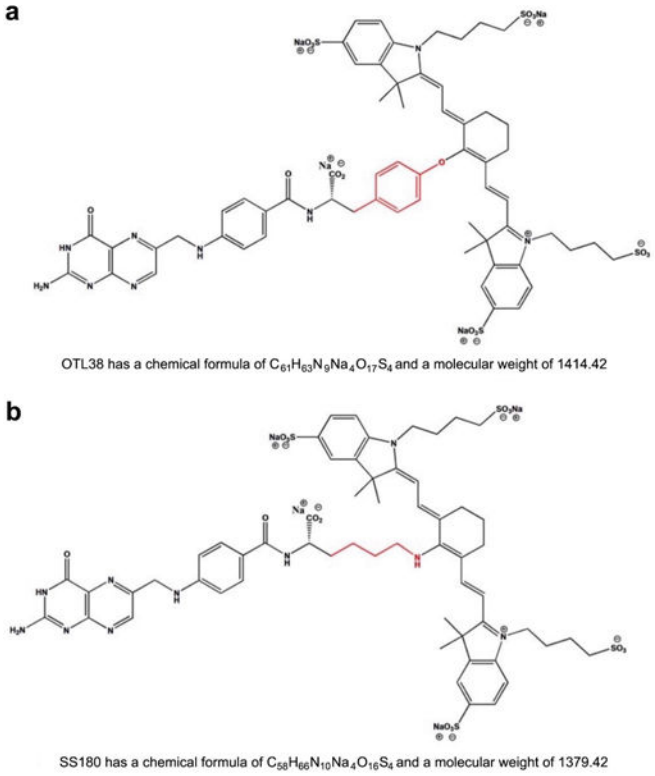

Figure 1.

Chemical formula, structure, and molecular weight of **a** OTL38 and **b** SS180 reveals a highly conserved structure with variation only in the cross-link between the folate ligand and cyanine backbone dye (red)

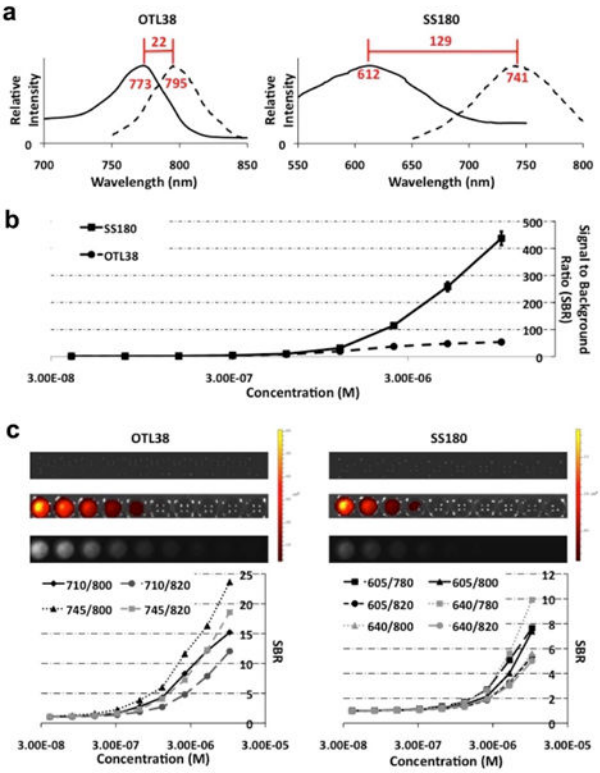

Figure 2.

a Excitation and emission spectra of OTL38 (Ex: 773 nm, Em: 795 nm, Stokes Shift: 22 nm) and SS180 (Ex: 612 nm, Em: 741 nm, Stokes Shift: 129 nm); **b** Serial concentrations of OTL38 and SS180 were analyzed using fluorometry with peak fluorescence intensities of OTL38 and SS180 at optimal fluorescence parameters demonstrating greater signal to background ratio (SBR) for SS180 compared with OTL38 (437 vs. 54, $p < 0.0001$); Serial concentrations of the dyes were used to optimize fluorescence parameters for both dyes with the In Vitro Imaging System (IVIS). **c** Optimal parameters for OTL38 (Ex: 745 nm, Em: 800 nm) and SS180 (Ex: 640 nm, Em: 780 nm) with average SBRs of OTL38 at least twice that of SS180 at each concentration for the optimized parameters.

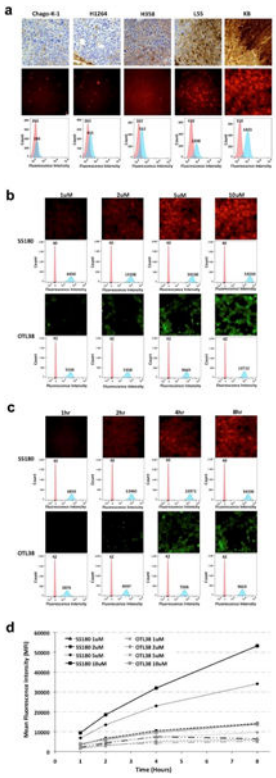

Figure 3.

a Correlation of immunohistochemistry, fluorescence microscopy, and flow cytometry demonstrates binding of SS180 correlates with FRα expression (by row: FRα staining, SS180 fluorescence microscopy, SS180 flow cytometry, values reported as mean fluorescence intensity [MFI]); **b** Dose- and **c** Time-dependent binding of SS180 and OTL38 to FRα; **d** Summary graph of MFI over dose and time for SS180 and OTL38

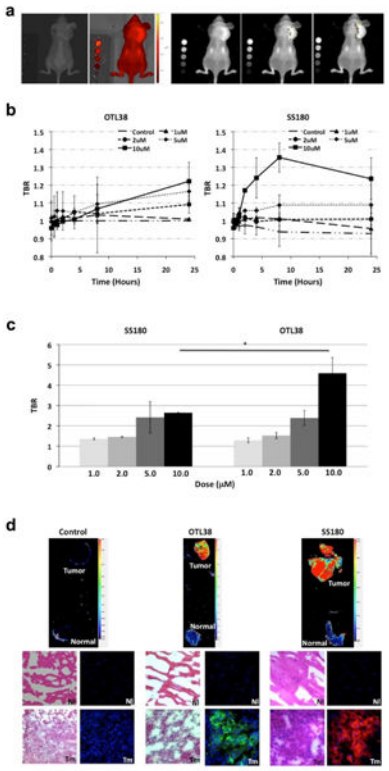

Figure 4.

a Sample IVIS images and TBR processing using ImageJ of murine flank tumor model for mice treated with OTL38 or SS180 systemically. Left to Right: black and white view, fluorescence heat map, fluorescence, estimation of tumor fluorescence, and estimation of background fluorescence; **b** Maximum TBR of OTL38 and SS180 *in vivo* reveals peak TBR of 1.22 for OTL38 treated mice at 10 μM, 24 h after injection and of 1.35 for SS180 treated mice at 10 μM, 8 h after injection ($p = 0.0806$). **c** *Ex vivo* assessment of harvested flank tumors reveals OTL38 treated mice had a higher peak TBR than SS180 treated mice (4.59 vs. 2.64, $p = 0.0210$); **d** Cross-sectional imaging of tumors and normal muscle tissue in dye-naïve, OTL38 treated mice and SS180 treated mice reveals OTL38 and SS180 accumulates on the tumor (Tm) cell surface but not on normal tissue (Nl – muscle).

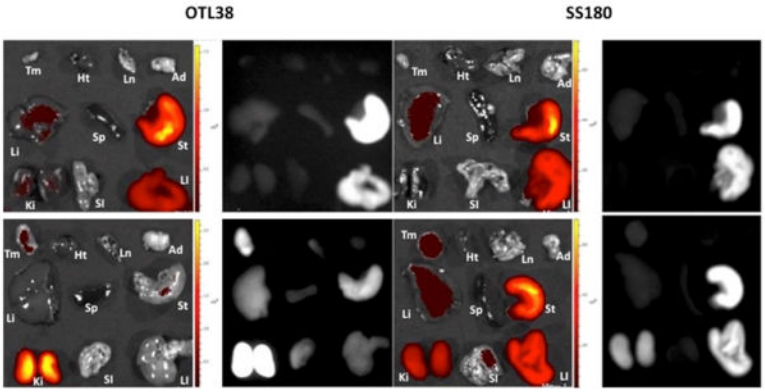

Figure 5.

Biodistribution and systemic toxicity studies of mice after injection with 100 μL of 10 μM OTL38 or SS180. Top Row, Dye-Naïve Mice; Bottom Row, Treatment Mice. Tm = Tumor, Ht = Heart, Ln = Lung, Ad = Adipose, Li = Liver, Sp = Spleen, St = Stomach, Ki = Kidney, SI = Small Intestine, LI = Large Intestine. Dye-Naïve Mice were imaged at OTL38 and SS180 IVIS parameters for complete comparison.

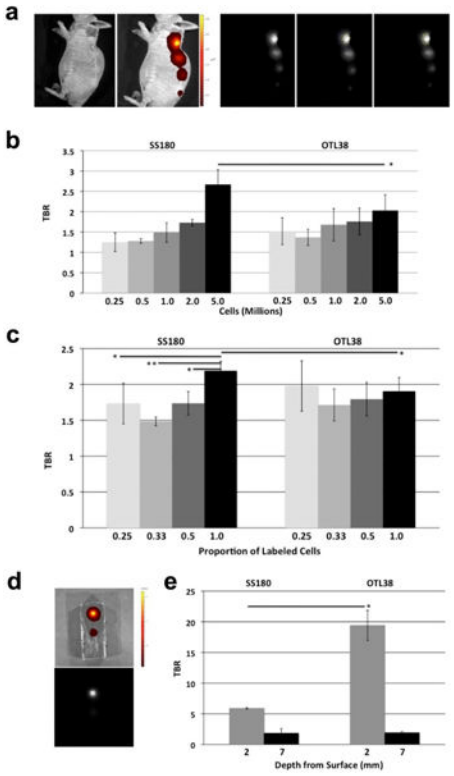

Figure 6.

a Sample IVIS images and TBR processing using ImageJ of subcutaneous injection model for mice injected with OTL38 or SS180 incubated cells. Left to Right: black and white view, fluorescence heat map, fluorescence, estimation of cell injection fluorescence, and estimation of background fluorescence; **b** Subcutaneous injection of SS180 incubated cells has a greater TBR compared with OTL38 incubated cells at 5×10^6 cells ($p = 0.05$), the minimum number of cells necessary to generate a TBR > 2 with either dye; **c** Subcutaneous injection of OTL38 and SS180 incubated cells mixed with unlabeled cells shows unlabeled cells do not alter the TBR of labeled cells in OTL38 (25% labeled cells, TBR = 1.97 vs. 100% labeled cells, TBR = 1.90, $p = 0.617$; 33% labeled cells, TBR = 1.71 vs. 100% labeled cells, TBR = 1.90, $p = 0.1635$; 50% labeled cells, TBR = 1.79 vs. 100% labeled cells, TBR = 1.90, $p = 0.2818$), but unlabeled cells dilute fluorescence signal strength in SS180 incubated cells (25% labeled cells, TBR = 1.73 vs. 100% labeled cells, TBR = 2.18, $p = 0.0322$; 33% labeled cells, TBR = 1.48 vs. 100% labeled cells, TBR = 2.18, $p = 0.0005$; 50% labeled cells, TBR = 1.73 vs. 100% labeled cells, TBR = 2.18, $p = 0.0103$); **d** Sample IVIS images of phantom depth model with fluorescence heat map (top) and fluorescence (bottom); **e** Dye fluorescence in phantom model showed significantly higher fluorescence for superficial dye deposits at 2 mm with OTL38 compared with SS180 (19.41 vs. 5.91, $p = 0.0159$), but not at deeper dye deposits of 7 mm (1.92 vs. 1.82, $p = 0.8696$). OTL38 and SS180 were not detected at a depth of 12 mm.